Supplementary Material

Grain boundaries assisting generation abundant Cu^+ for highly selective electro-reduction CO_2 to ethanol

Xinze Bi[a], Yuezhu Zhao[a], Yifan Yan[a], Hongzhi Wang[*,b], Mingbo Wu[*,a]

a.College of New Energy, College of Chemical Engineering, State Key Laboratory of Heavy Oil Processing, China University of Petroleum (East China), Qingdao 266580, China

b.College of Chemistry and Chemical Engineering, Ocean University of China, Qingdao, 266100, China

*Corresponding author. Email: wumb@upc.edu.cn; wanghz@ouc.edu.cn.

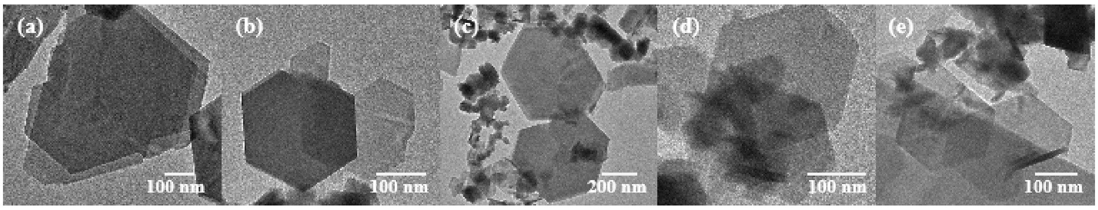

Fig. S1. (a-e) The TEM images of $CuSe^{X}$ (X=1, 2, 3, 4, 5), respectively.

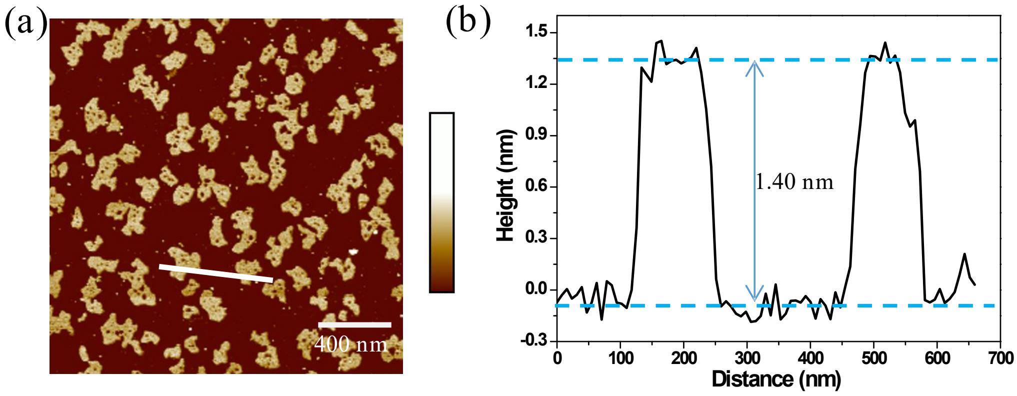

Fig. S2. (a, b) The AFM characterization of CuSe[3].

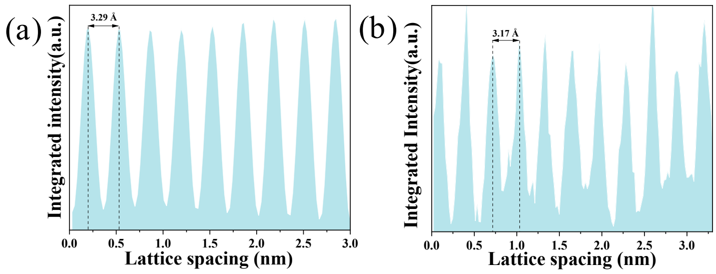

Fig. S3. The lattice spacing obtained by integrating a few atomic layers of Cu_7Se_4(222)(a) and CuSe(102)(b).

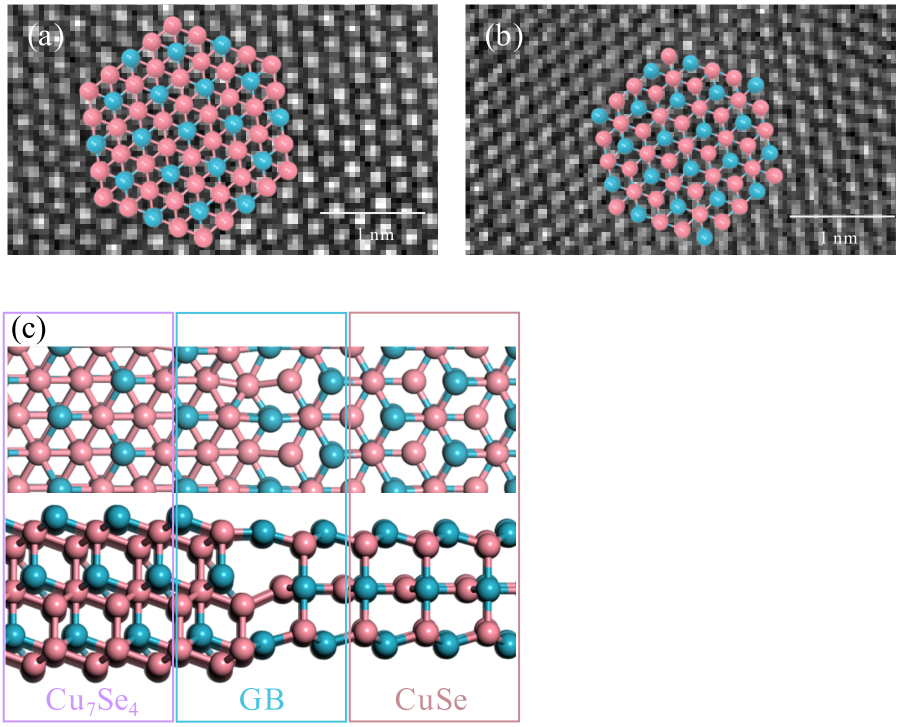

Fig. S4. The HRTEM images of Cu_7Se_4(a) and CuSe(b). (c) Top view and of front view of the model of CuSe[3].

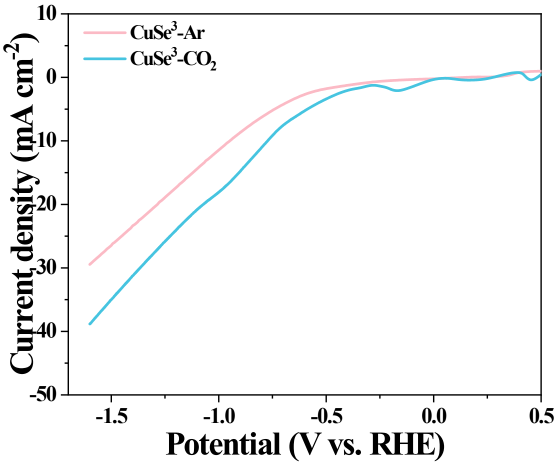

Fig. S5. Linear sweep voltammetry curves toward CO_2ER at different atmospheres for $CuSe^3$.

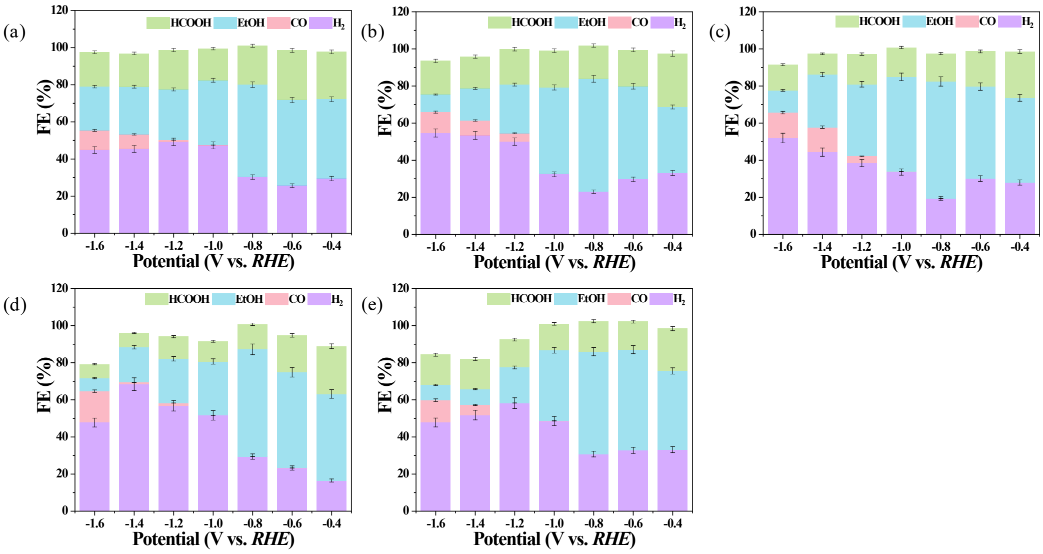

Fig. S6. (a-e) FEs and product distributions for $CuSe^X$.

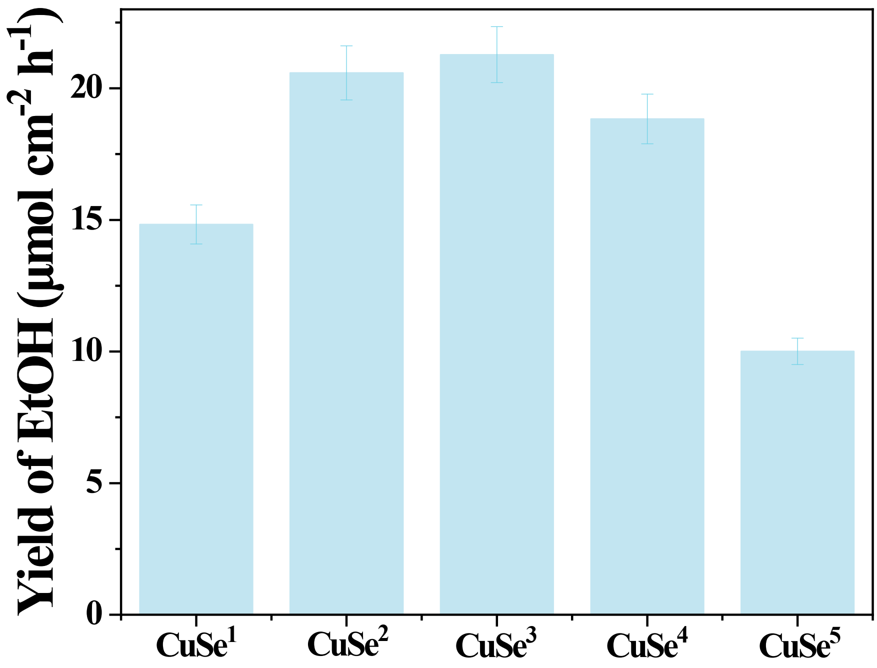

Fig. S7. Yield of EtOH for $CuSe^{X}$.

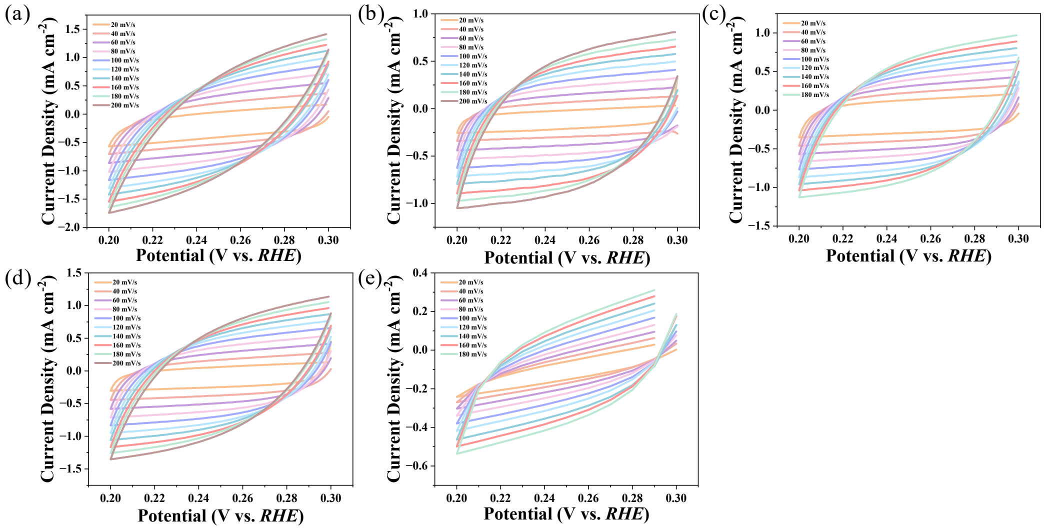

Fig. S8. (a-e) Cyclic voltammograms for $CuSe^{X}$.

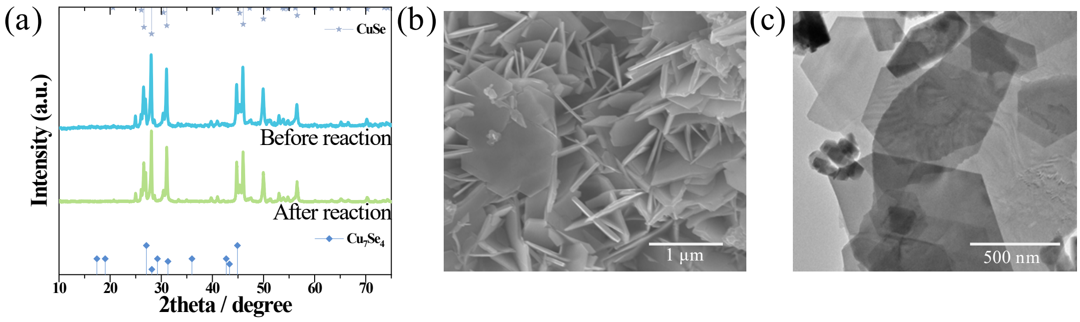

Fig. S9. (a) XRD patterns, (b) the SEM image and (c) the TEM image for CuSe[3] after 8 h CO_2ER at −0.8 V *vs.* RHE.

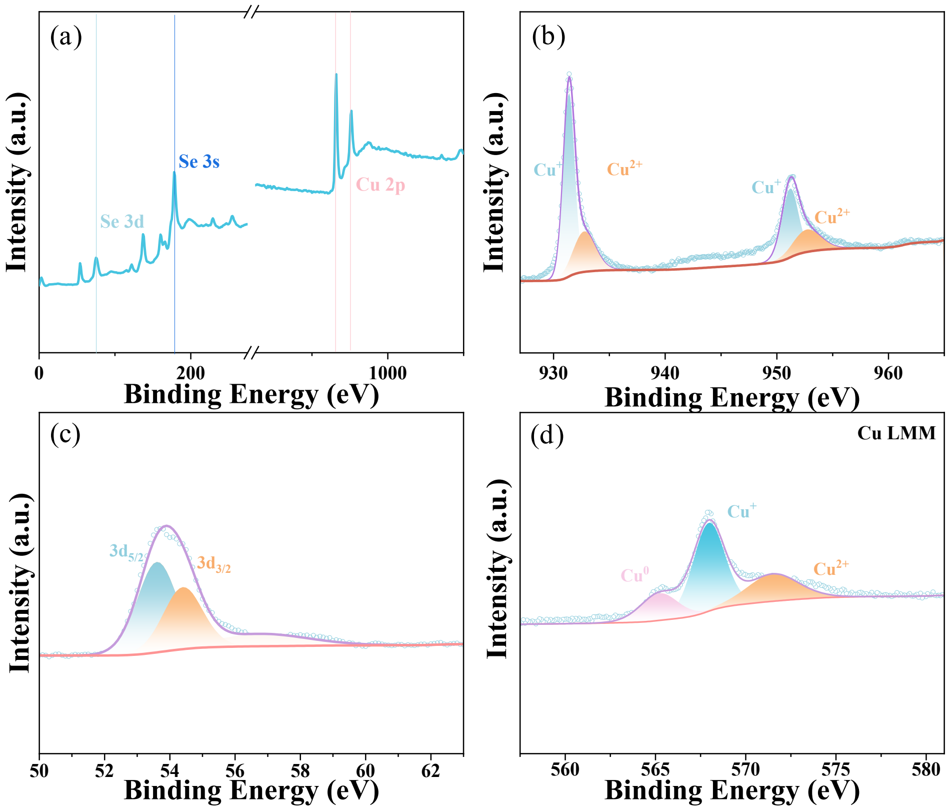

Fig. S10. (a) Total XPS curve, (b) Cu 2p XPS curve, (c) Se 3d XPS curve and (d) Cu LMM Auger spectra.

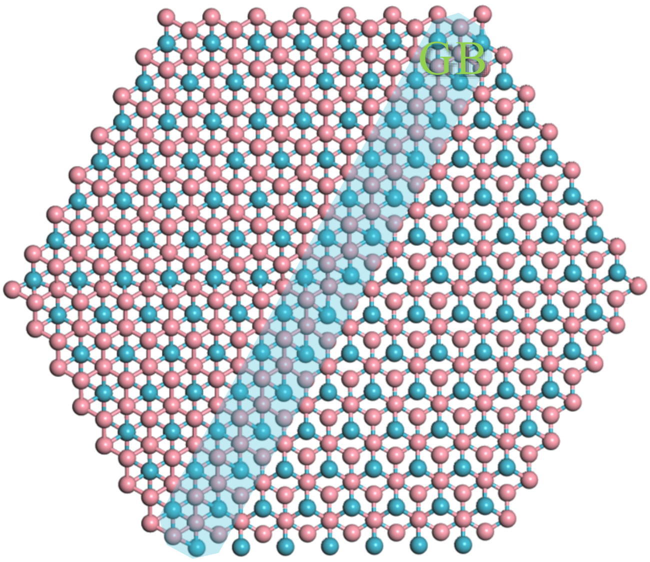

Fig. S11. The model for GB.

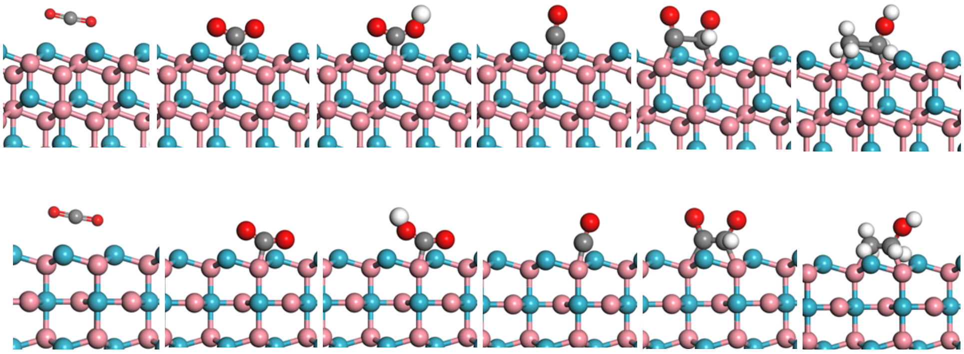

Fig. S12. The model of free energy for Cu_7Se_4 and CuSe.

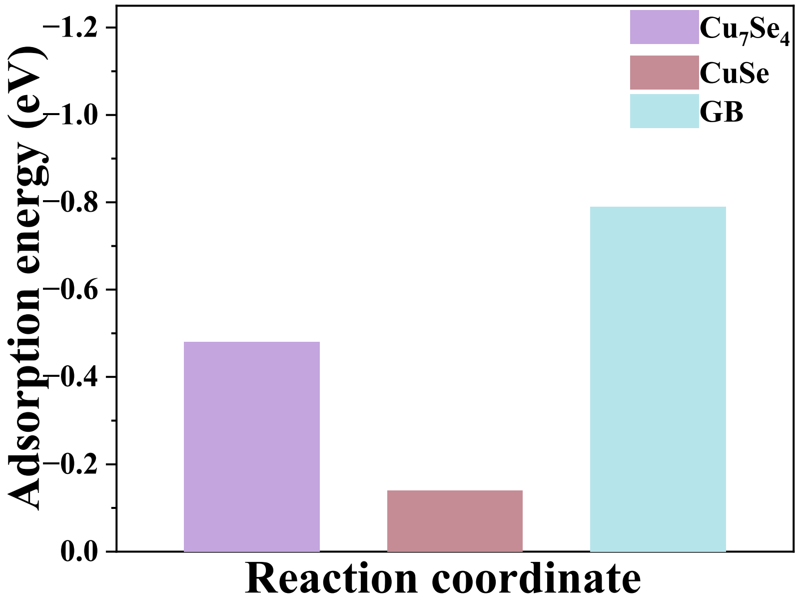

Fig. S13. Adsorption energy of *CO intermediate on CuSe[3].

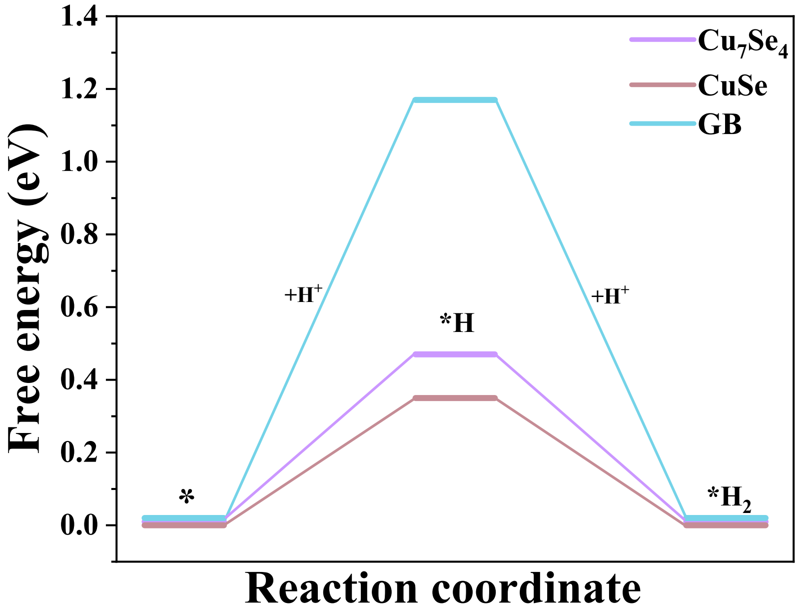

Fig. S14. Free energy diagram for H_2 on CuSe[3].

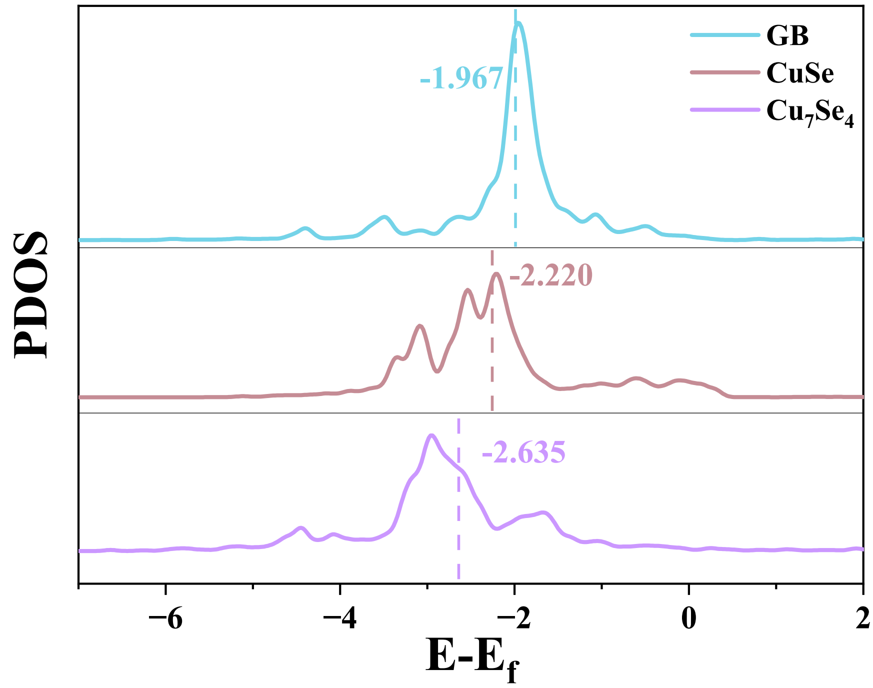

Fig. S15. Calculated d-projected density of states (PDOS) of surface Cu atoms on CuSe[3].

Tab. S1. EDX data of $CuSe^X$.

Sample	Cu/at%	Se/at%
$CuSe^1$	90.72	9.28
$CuSe^2$	82.21	17.79
$CuSe^3$	65.79	34.21
$CuSe^4$	59.70	40.30
$CuSe^5$	51.39	48.61

Tab. S2. Element content of Cu and Se from the total XPS spectra for $CuSe^{X}$.

Sample	Se/at%	Cu/at%
$CuSe^{1}$	30.82	69.18
$CuSe^{2}$	38.19	61.81
$CuSe^{3}$	41.68	58.32
$CuSe^{4}$	48.94	51.06
$CuSe^{5}$	56.66	43.34

Tab. S3. Distribution for Cu chemical states from the Cu 2p XPS spectra for $CuSe^X$.

Cu 2p	$2P_{3/2}$		$2P_{1/2}$		$(Cu^{+}+Cu^{0})/Cu^{2+}$
	Cu^{+}/Cu^{0}	$Cu^{2}+$	Cu^{+}/Cu^{0}	Cu^{2+}	
$CuSe^1$	42.61%	21.41%	23.76%	12.22%	1.97
$CuSe^2$	31.38%	25.40%	36.63%	6.59%	2.13
$CuSe^3$	45.35%	20.11%	26.42%	8.12%	2.54
$CuSe^4$	28.42%	28.77%	35.09%	7.72%	1.74
$CuSe^5$	25.50%	40.18%	11.36%	22.96%	0.58

Tab. S4. The fitted results of EIS for $CuSe^X$.

Sample	Rs	1-CPE-T	1-CPE-P	Rct	2-CPE-T	2-CPE-P	Rct
$CuSe^1$	0.15	7.76E-7	0.99	16.00	7.36E-3	0.46	697.80
$CuSe^2$	0.26	6.09E-7	0.80	23.55	6.79E-3	0.61	1256.00
$CuSe^3$	0.25	7.21E-7	0.83	21.18	7.30E-3	0.67	370.70
$CuSe^4$	0.29	5.41E-7	0.84	22.32	2.02E-3	0.74	834.70
$CuSe^5$	0.16	5.29E-7	0.85	18.99	3.47E-3	0.76	792.30

Tab. S5. Distribution for Cu chemical states from the Cu 2p XPS spectra and Cu LMM Auger spectra for $CuSe^3$.

Cu 2p	$2P_{3/2}$		$2P_{1/2}$		$(Cu^{+}+Cu^{0})/Cu^{2+}$
	Cu^{+}/Cu^{0}	Cu2+	Cu^{+}/Cu^{0}	Cu^{2+}	
$CuSe^3$	43.64%	18.96%	24.10%	13.30%	2.10

Tab. S6. Distribution for Cu chemical states from the Cu LMM Auger spectra for $CuSe^3$.

	Cu^0	Cu^+	Cu^{2+}
$CuSe^3$	19.48%	53.70%	26.82%